

Three-Dimensional MHD Analysis of Heliotron Plasma with RMP

**K. Ichiguchi^{1,2)}, Y. Suzuki^{1,2)}, M. Sato¹⁾, Y. Todo^{1,2)}, T. Nicolas¹⁾,
S. Sakakibara^{1,2)}, S. Ohdachi^{1,2)}, Y. Narushima^{1,2)}, and B.A.Carreras³⁾**

National Institute for Fusion Science, Japan¹⁾

The graduate University of Advance Study, SOKENDAI, Japan²⁾

Universidad Carlos III, Spain³⁾

**25th IAEA Fusion Energy Conference (FEC2014),
St Petersburg, Russian Federation, 13-18 October 2014**

Acknowledgements

This work is supported by the budget NIFS14KNST063 of National Institute for Fusion Science, and Grant-in-Aid for Scientific Research (C) 22560822 of Japan Society for Promotion Science. Plasma simulator (NIFS) and Helios(IFERC-CSC) were utilized for the calculations.



1. Introduction

Motivation of this study

Coil Configuration of Large Helical Device (LHD)

2. Three-dimensional equilibrium including resonant magnetic perturbation (RMP)

Numerical Scheme of HINT2 code

Difference of magnetic surfaces and pressure profiles
between with and without RMP

3. Effects of RMP on pressure-driven mode dynamics

Simulation procedure of MIPS code

RMP dependence of linear modes

- difference in the mode structure

Comparison of nonlinear dynamics with and without RMP

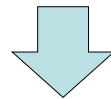
- difference in the spatial phase in the collapse

Relation with LHD experiments

4. Summary

- Effects of RMPs have been extensively studied in toroidal confinement experiments.
 - Tokamaks : Relaxation of the pressure gradient at pedestal region is studied for the mitigation of ELMs.
(e.g. Evans et al. Nature Phys. 2006)
 - Stellarator (LHD) : Penetration into the plasma and the effects on the global stability are studied.
(e.g. Sakakibara et al. NF 2013)

- Numerical MHD analyses of the effects of RMPs have also progressed.
 - However, in most of previous numerical analyses for RMPs, equilibria with nested flux surfaces are employed, and then, RMPs are applied on the equilibria.
(e.g. Garcia et al. NF2003, Strauss et al. NF2009, Saito et al. PoP2010, Becoulet et al. NF2012)
 - The initial pressure profile corresponding to the nested surfaces is **inconsistent** with the magnetic field including the RMPs.
 - In order to incorporate the pressure profile **consistent** with the magnetic field, **three-dimensional (3D) analyses including RMPs** are indispensable.



- Here, we analyze the effects of **RMPs on pressure driven modes** in the **Large Helical Device (LHD)** by utilizing **3D equilibrium and dynamics codes**.

- ◆ Large Helical Device (LHD)

is a typical heliotron device composed of helical coils and poloidal field coils.

- ◆ Coil configurations

Helical coils

Pole number : 2

Field period : 10

Poloidal coils

3 pairs

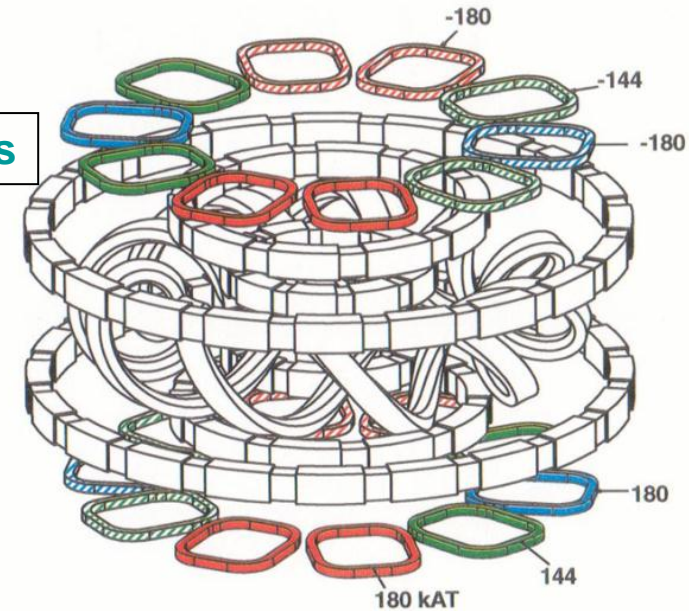
RMP coils

- ◆ No net toroidal current is needed.

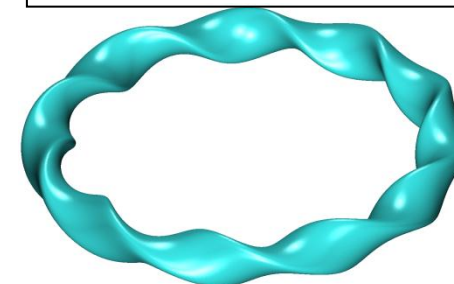
Plasma is stable for current driven modes.

Pressure driven modes are the most dangerous.

- ◆ RMPs are controlled by the currents in 10 pairs of RMP coils.



Typical LHD Plasma



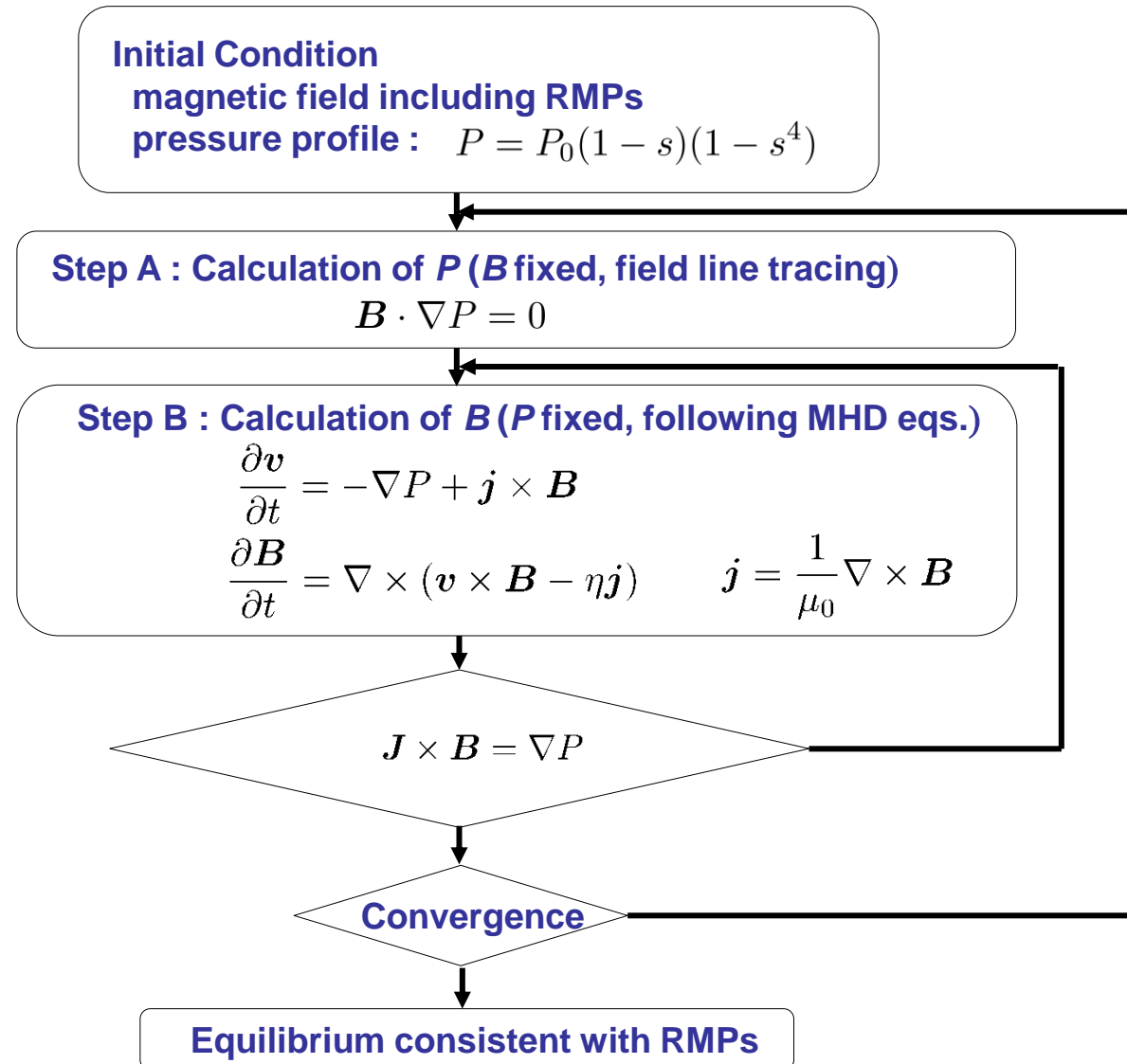
3D Equilibrium Calculation



● HINT2 code

(Y. Suzuki, et al.,
Nuclear Fusion (2006) L19)

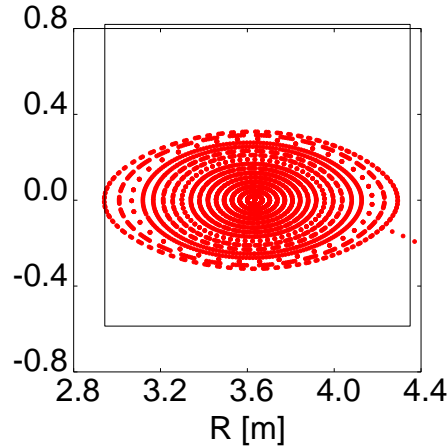
- The HINT2 code solves the 3D equilibrium equations without any assumptions of the existence of the nested flux surfaces. (suitable for the equilibrium analysis including RMPs)
- An LHD configuration with an inwardly shifted vacuum magnetic axis and a high aspect ration is employed. (Rax=3.6m, $\gamma=1.13$)
- Calculation starts with the parabolic pressure profile with $\beta_0 = 4.4\%$.



3D LHD Equilibrium (1)

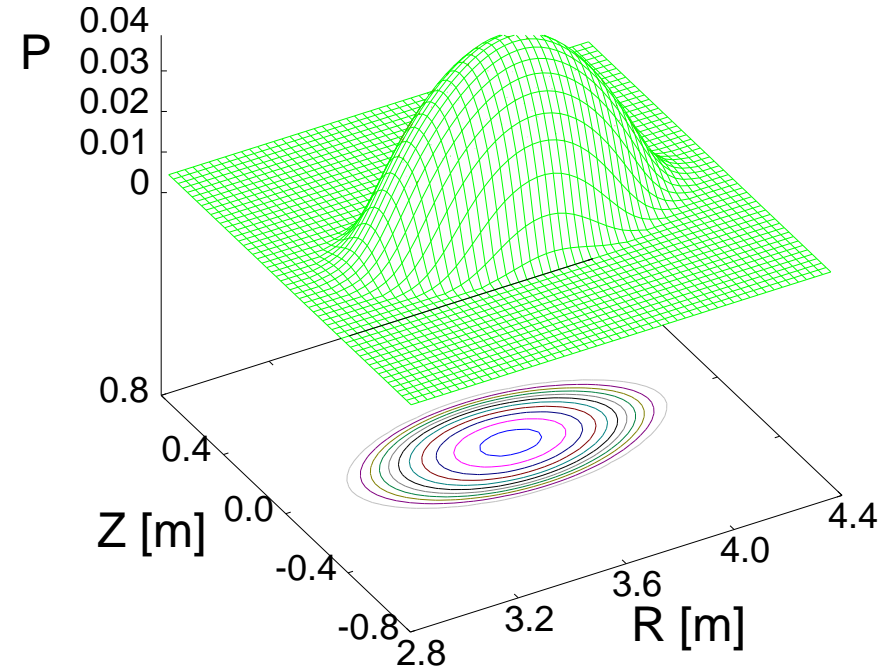
- Equilibrium **without RMP**

Puncture plot of field lines



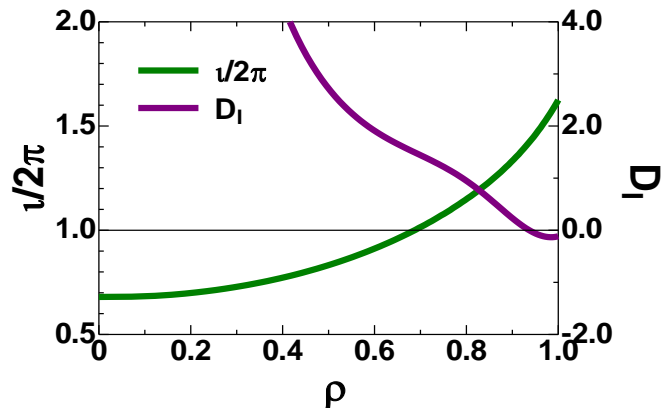
Nested surfaces
exist in the
whole plasma
region.

Bird's eye view and contour map of pressure



Pressure profile is smooth
and the contours are also nested
corresponding to the magnetic surfaces.

Rotational Transform & Mercier Stability

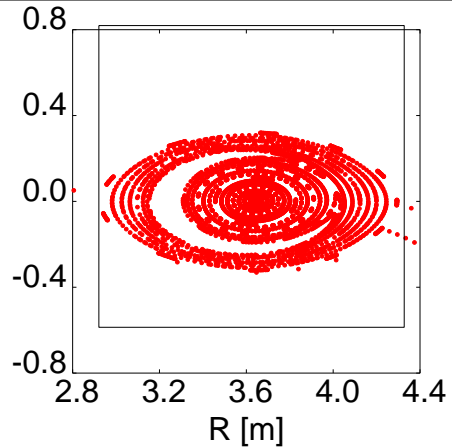


Rational surface of $1/2\pi=1$ exists in the plasma.
The $1/2\pi=1$ surface is **Mercier unstable**.

3D LHD Equilibrium (2)

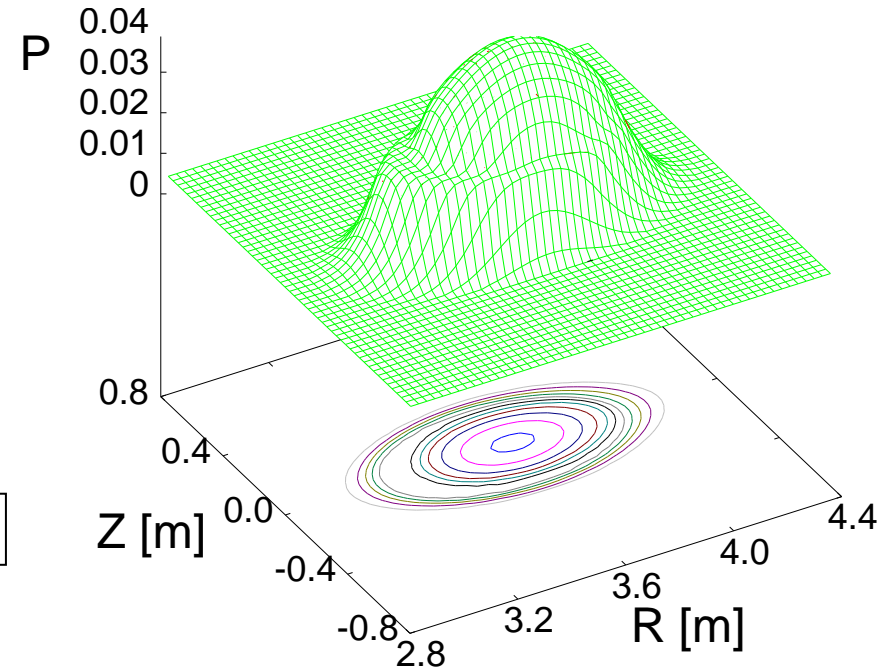
- **Equilibrium with a horizontally uniform RMP** ($\delta B/B_t = 3.0 \times 10^{-4}$)

Puncture plot of field lines

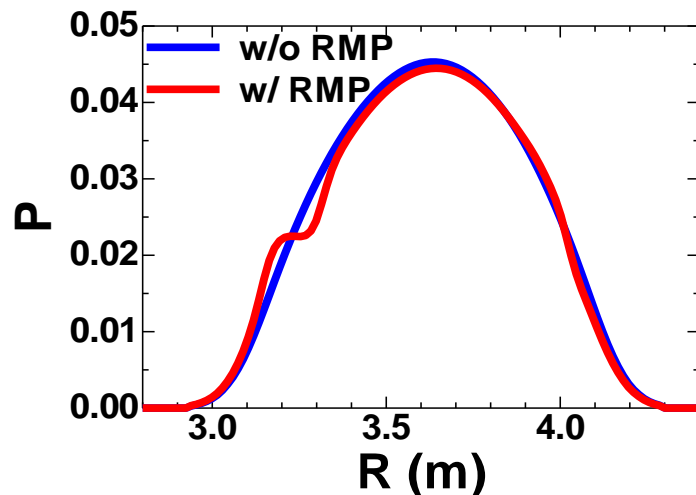


An $m=1/n=1$ magnetic island is generated by the resonance with the $\nu/2\pi=1$ field lines.

Bird's eye view and contour map of pressure



Comparison of pressure profile along Z=0 line



Shoulder like structure in the bird's eye view and island structure in the contour map are seen.

➡ **PRESSURE CONSISTENT with RMP**

Pressure profile is locally flat at the O-point, while the profile is steep at the X-point.

- **MIPS code** (Todo et al., Plasma Fus. Res. (2010) S2062)
 - Solves the full MHD equations by following the time evolution.
 - 4th order central difference method for (R, ϕ , Z) directions.
 - 4th order Runge Kutta scheme for the time evolution.
 - The most unstable mode is detected.

Basic equations

$$\frac{\partial \rho}{\partial t} = -\nabla \cdot (\rho \mathbf{v})$$

$$\frac{\partial \mathbf{v}}{\partial t} = -\rho \boldsymbol{\omega} \times \mathbf{v} - \rho \nabla \left(\frac{v^2}{2} \right) - \nabla p + \mathbf{j} \times \mathbf{B} + \frac{3}{4} \nabla [\nu \rho (\nabla \cdot \mathbf{v})] - \nabla \times (\nu \rho \boldsymbol{\omega})$$

$$\frac{\partial \mathbf{B}}{\partial t} = -\nabla \times \mathbf{E}$$

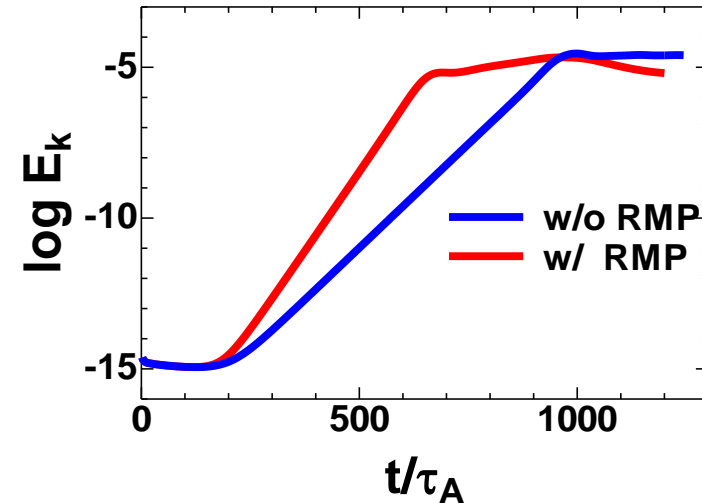
$$\frac{\partial p}{\partial t} = -\nabla \cdot (p \mathbf{v}) - (\Gamma - 1) p \nabla \cdot \mathbf{v} + \chi_{\perp} \nabla_{\perp}^2 (p - p_{eq}) + \chi_{\parallel} \nabla_{\parallel}^2 p$$

$$\mathbf{E} = -\mathbf{v} \times \mathbf{B} + \eta (\mathbf{j} - \mathbf{j}_{eq})$$

$$\mathbf{J} = \frac{1}{\mu_0} \nabla \times \mathbf{B}$$

$$\boldsymbol{\omega} = \nabla \times \mathbf{v}$$

Typical time evolution of kinetic energy



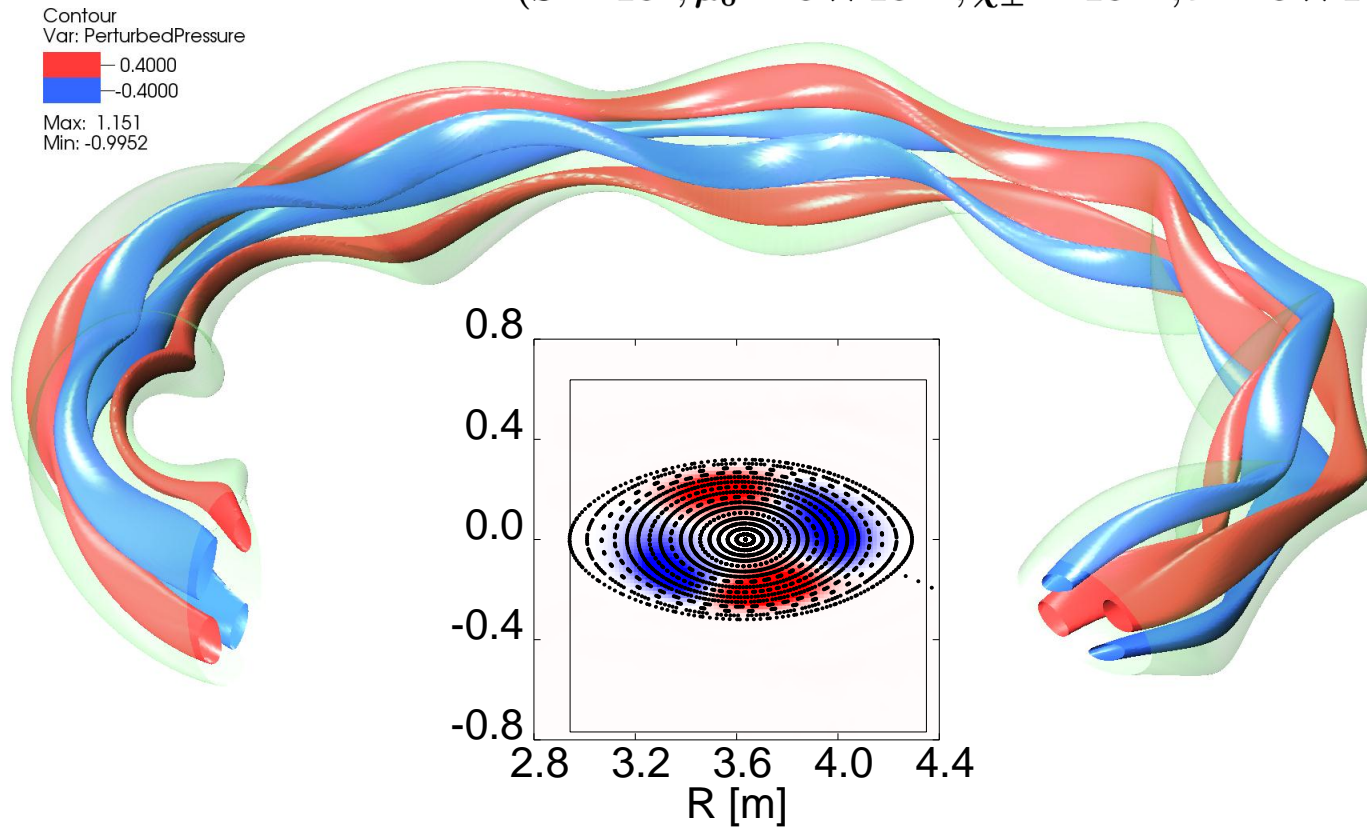
$$(S = 10^6, \mu_0 = 6 \times 10^{-5}, \chi_{\perp} = 10^{-6}, \nu = 6 \times 10^{-5}, \chi_{\parallel} = 10^{-3})$$

In either case, a pressure driven mode grows. After the linear phase, the modes are saturated nonlinearly.

- Mode structure **without RMP**

Mode pattern of perturbed pressure

$$(S = 10^6, \mu_0 = 6 \times 10^{-5}, \chi_{\perp} = 10^{-6}, \nu = 6 \times 10^{-5}, \chi_{\parallel} = 10^{-3})$$



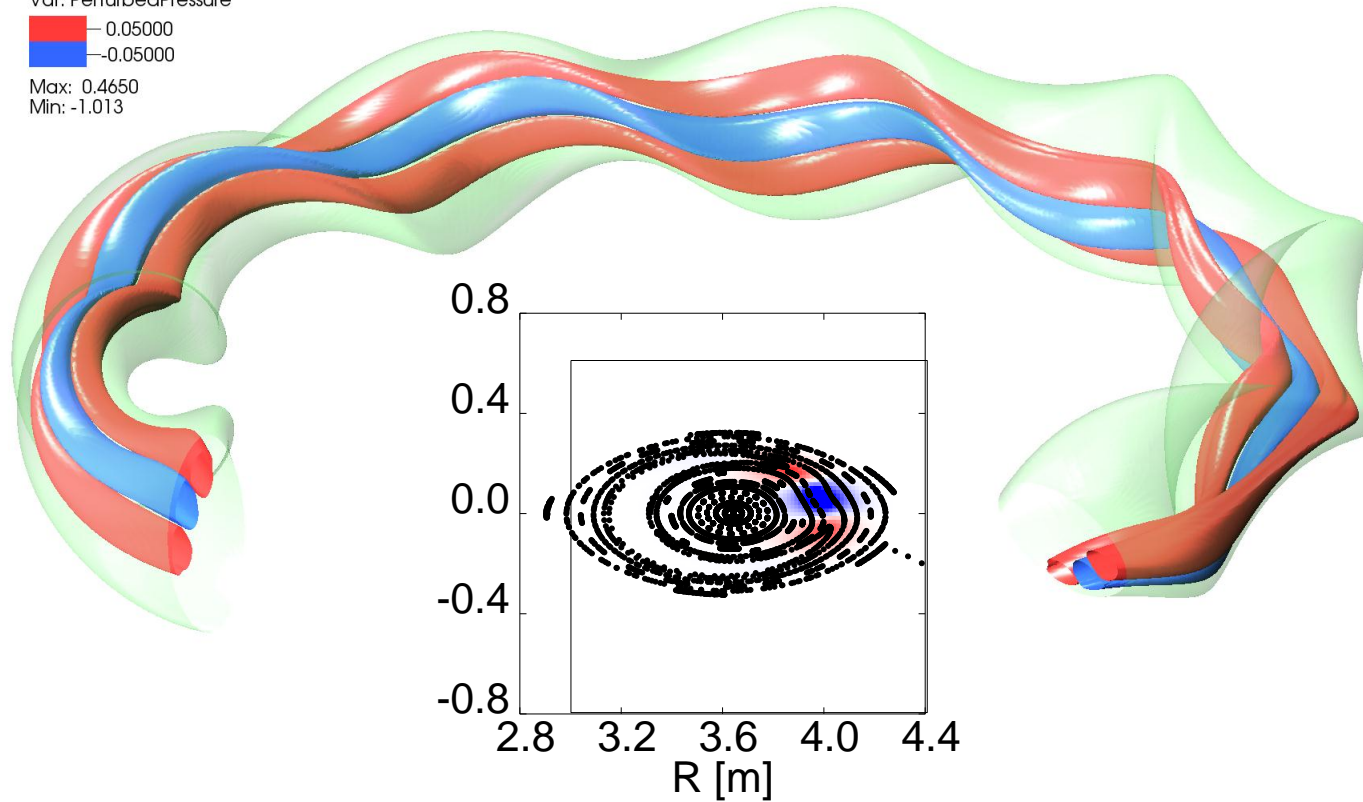
The mode pattern is distributed around the $\iota/2\pi=1$ surface almost uniformly. This pattern indicates that this mode is a **typical interchange mode**. The mode number is $m=2/n=2$ due to a fairly large viscosity.

- Mode structure **with RMP**

Mode pattern of perturbed pressure

$$(S = 10^6, \mu_0 = 6 \times 10^{-5}, \chi_{\perp} = 10^{-6}, \nu = 6 \times 10^{-5}, \chi_{\parallel} = 10^{-3})$$

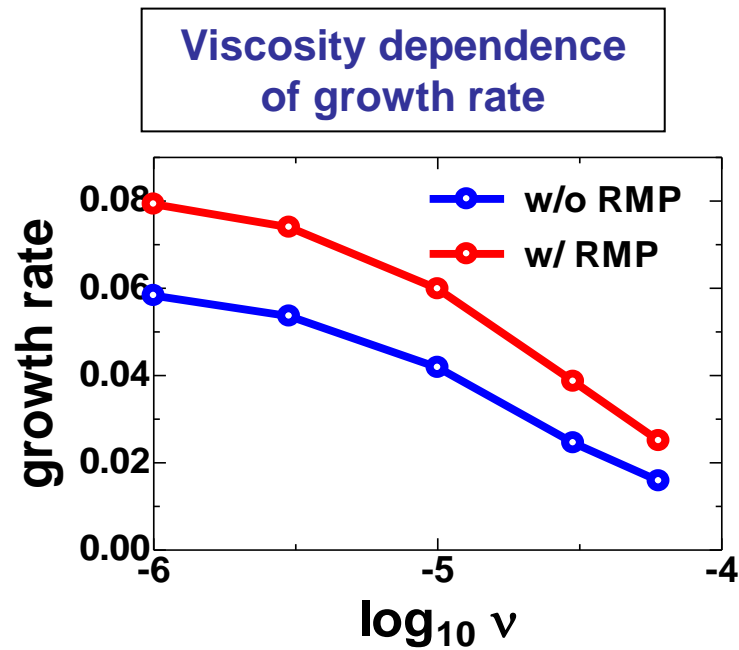
Contour
Var: PerturbedPressure
0.05000
-0.05000
Max: 0.4650
Min: -1.013



The mode is **localized around the X-point** showing a **ballooning-like structure**. This localization is due to the deformation of the equilibrium pressure profile. The mode can utilize the driving force the most effectively by being **localized around the steepest pressure gradient position**.

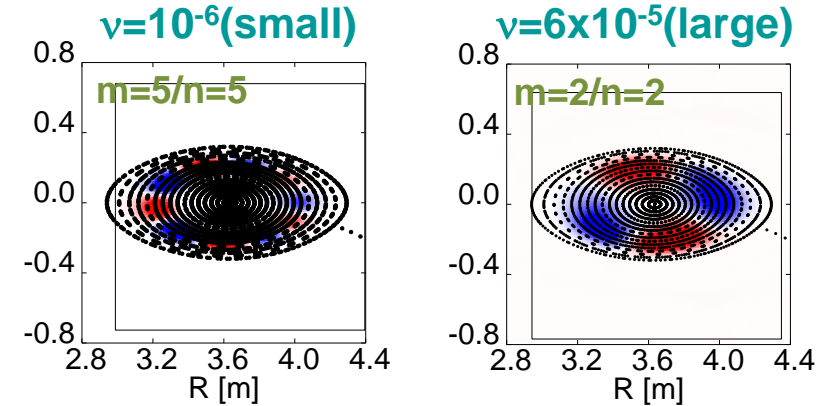
Viscosity Dependence of Linear Mode

- Components with the higher mode number is stabilized the more effectively.



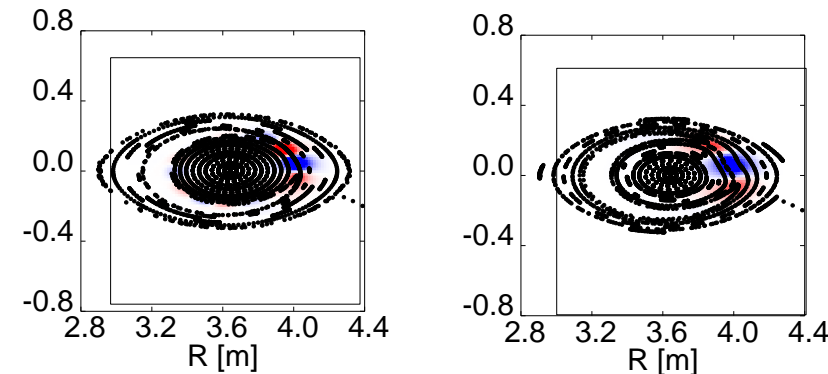
In both cases, the growth rates decrease as the viscosity increases. The amount of the decrease in the case with RMP is larger than that in the case without the RMP.

w/o RMP



Mode number of the most unstable interchange mode is just decreased by the increase of the viscosity.

w/ RMP

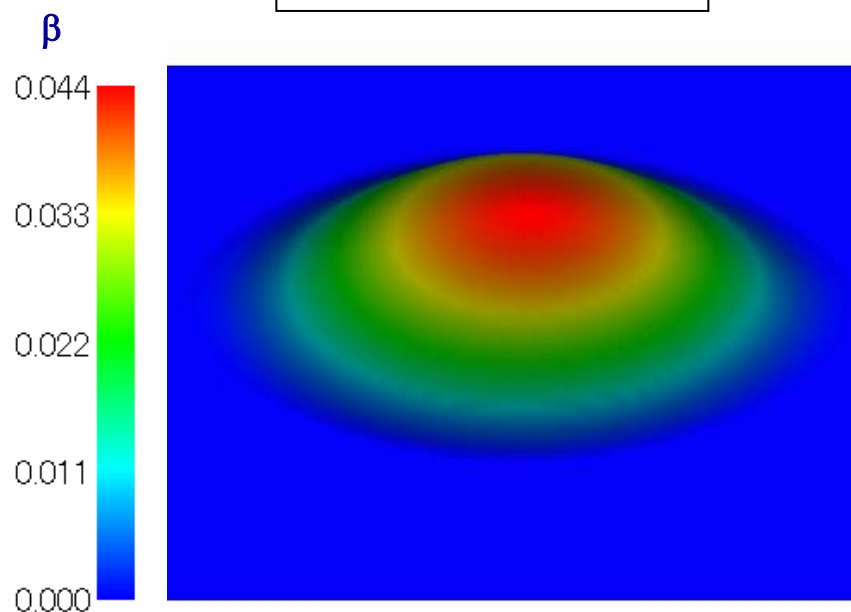


The mode structure is extended in the poloidal direction. This is due to the fact that the stabilization of the high mode components makes the localization weak. Since the mode structure extends to the small pressure gradient region, the reduction of the growth rate is enhanced.

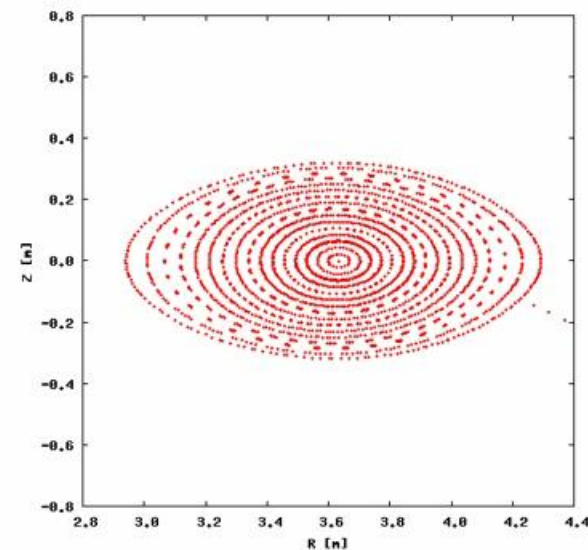
- Time evolution of pressure and magnetic surfaces in the case **without RMP**

$$(S = 10^6, \mu_0 = 6 \times 10^{-5}, \chi_{\perp} = 10^{-6}, \nu = 6 \times 10^{-5}, \chi_{\parallel} = 10^{-3})$$

Total Pressure



Puncture plot of field lines

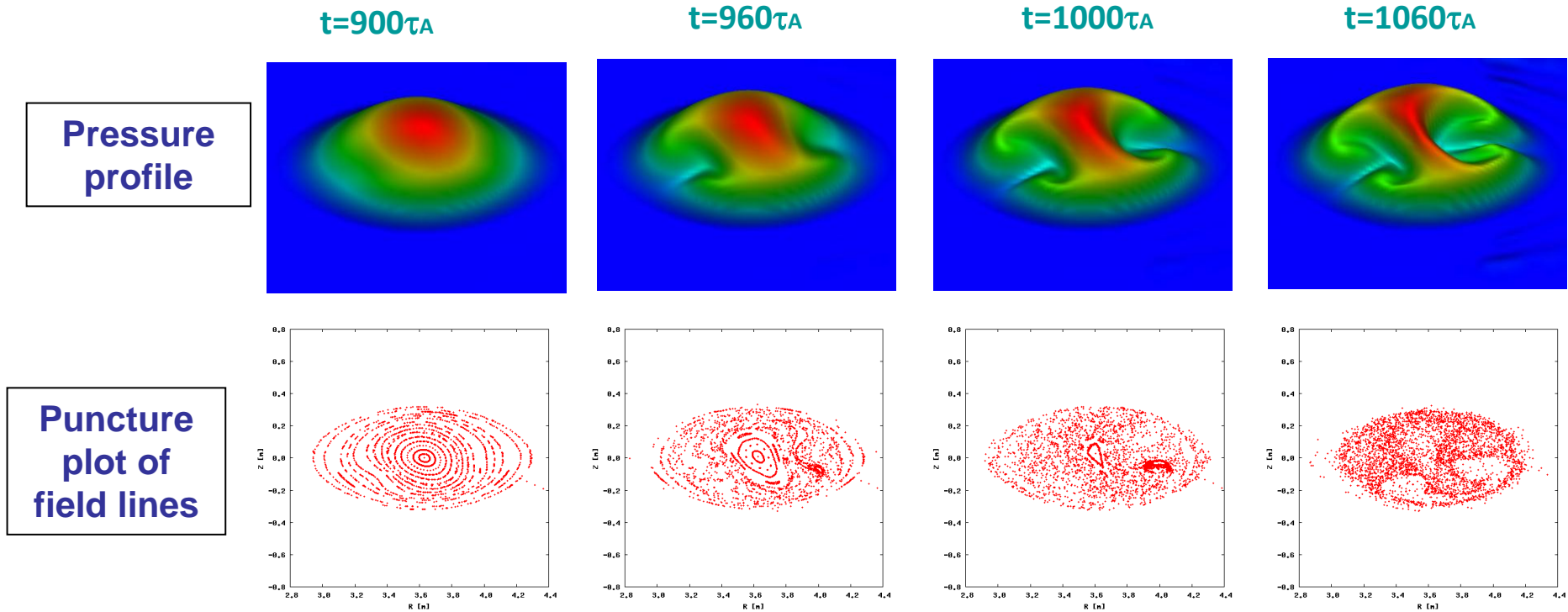


According to the linear mode structure, the $m=2/n=2$ interchange mode starts to evolve from the equilibrium with the smooth pressure profile and the nested surfaces, and leads to the collapse.

Snapshots without RMP

- Snapshots of pressure and field lines in the case **without RMP**

$$(S = 10^6, \mu_0 = 6 \times 10^{-5}, \chi_{\perp} = 10^{-6}, \nu = 6 \times 10^{-5}, \chi_{\parallel} = 10^{-3})$$



The convection of the interchange mode generates a mushroom-like structure, which leads to the collapse in the core region. The interchange mode can be destabilized with an arbitrary phase in the poloidal and the toroidal directions.

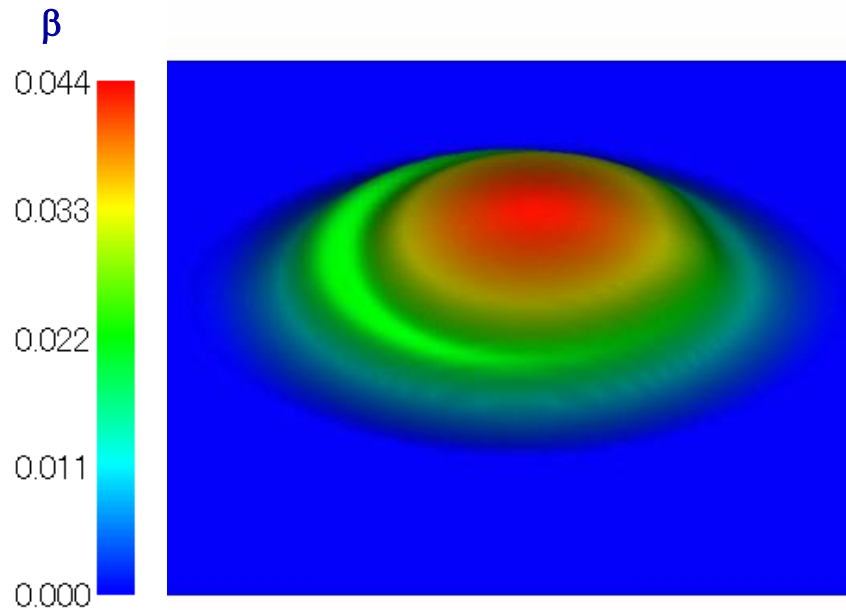


Spatial phase of the collapse can be changed.

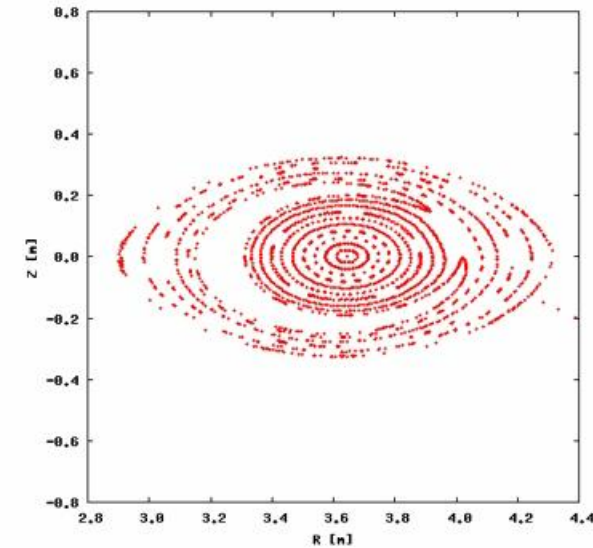
- Time evolution of pressure and magnetic surfaces in the case **with RMP**

$$(S = 10^6, \mu_0 = 6 \times 10^{-5}, \chi_{\perp} = 10^{-6}, \nu = 6 \times 10^{-5}, \chi_{\parallel} = 10^{-3})$$

Total Pressure



Puncture plot of field lines

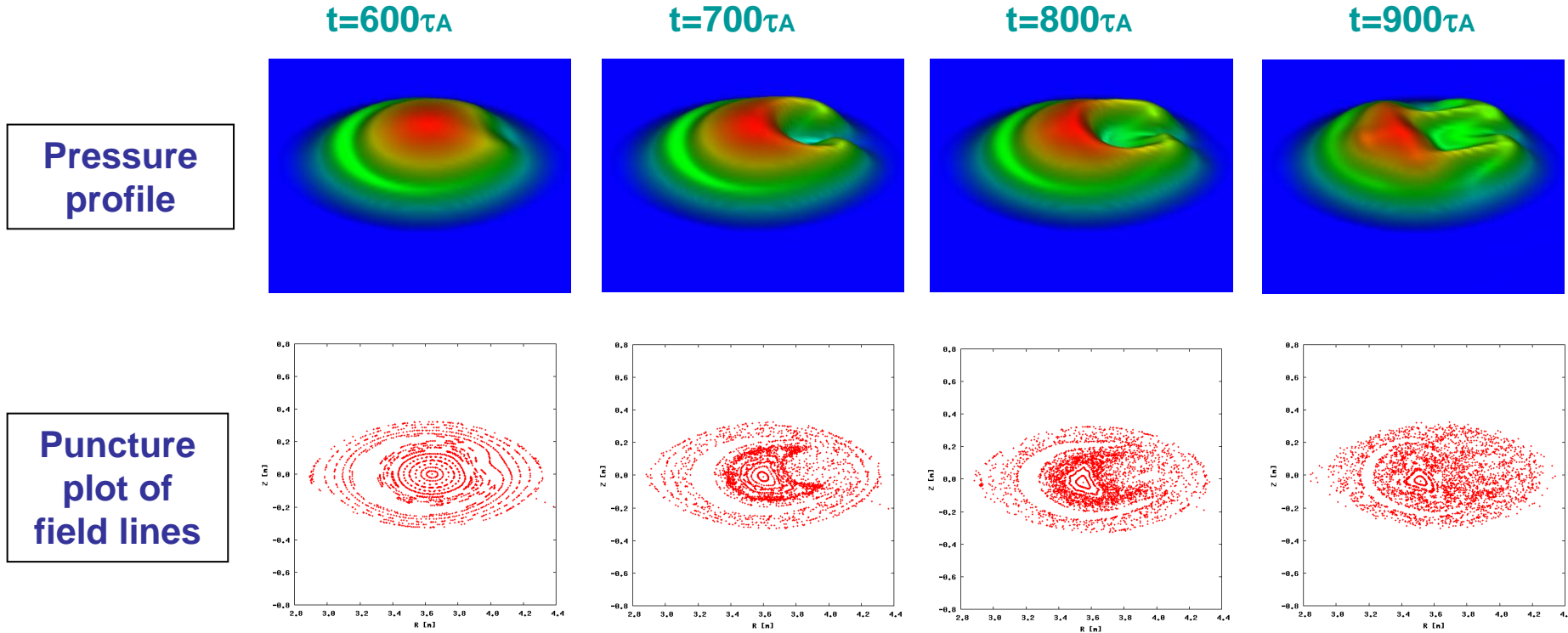


According to the linear mode structure, the ballooning-like mode starts to evolve from the equilibrium with the locally flattened pressure profile and the $m=1/n=1$ magnetic island, and leads to the collapse.

Snapshots with RMP

- Snapshots in nonlinear phase in the case **with RMP**

$$(S = 10^6, \mu_0 = 6 \times 10^{-5}, \chi_{\perp} = 10^{-6}, \nu = 6 \times 10^{-5}, \chi_{\parallel} = 10^{-3})$$



Pressure collapse occurs at the X-point initially, and expands toward the core region. Field line structure becomes stochastic also from the X-point, however, the O-point structure survives even in the large collapse of the pressure.



Spatial phase of the collapse should be fixed to the island.

Confirmation of Difference in Phase Property

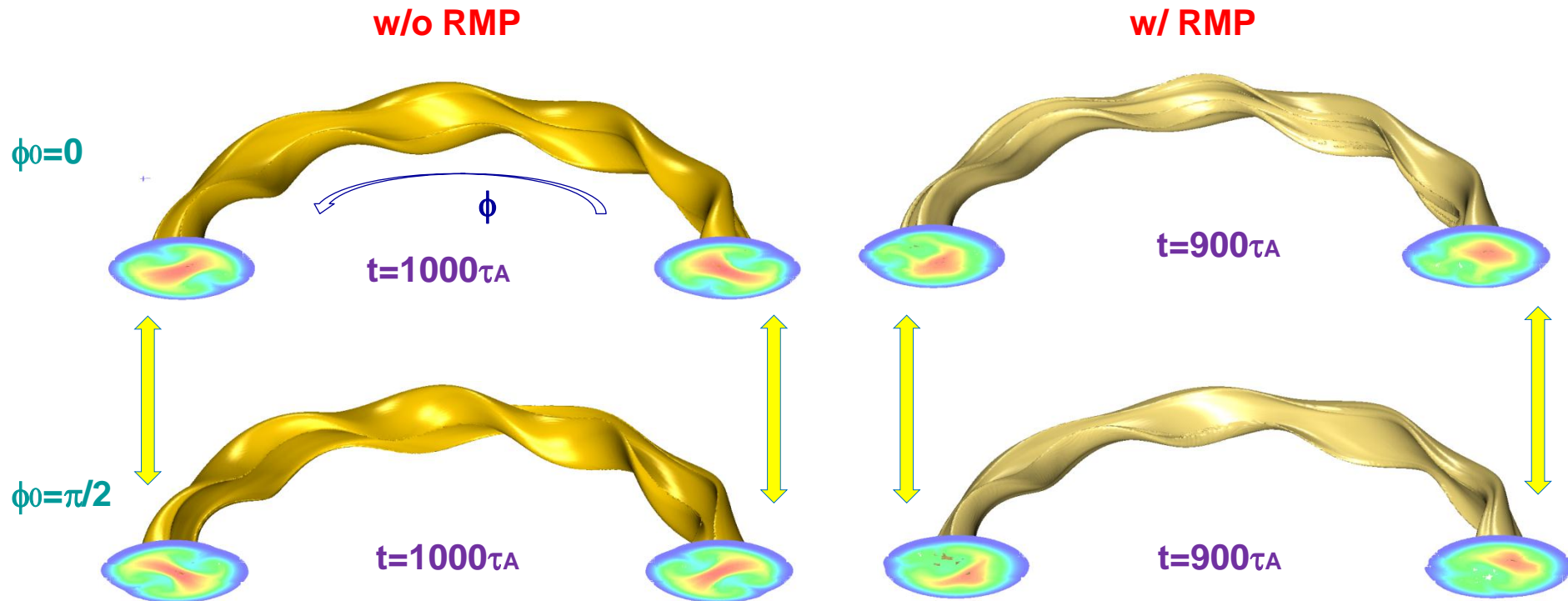


- Phase of the initial condition is changed for the confirmation.

Initial perturbations are given as $\tilde{X}_{ini} = \text{Rand}(\phi) \cos(\phi - \phi_0)$

$\left[\begin{array}{l} \text{Rand}(\phi) : \text{random function of toroidal angle} \\ \phi_0 : \text{initial toroidal phase} \end{array} \right.$

Constant pressure surface of $\beta=3.0\%$ and pressure contour at enlarged cross section (x1.5)

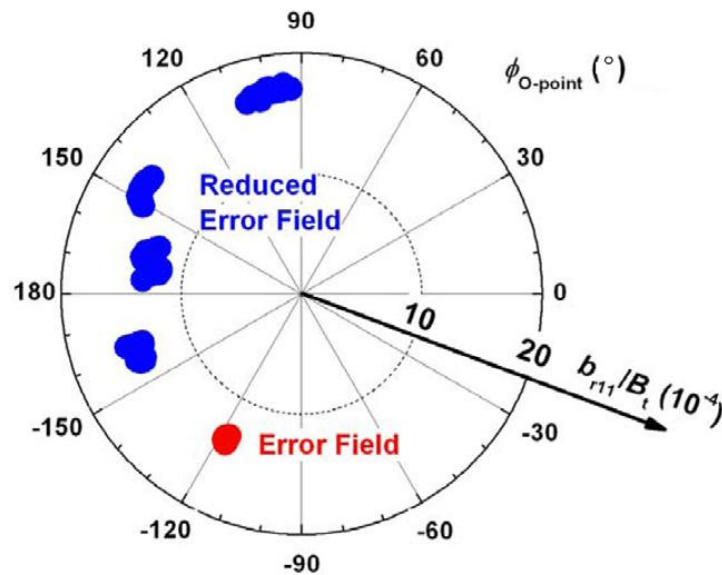


Collapse phase can change depending on the initial phase.

Collapse phase is fixed independent of the initial phase.

- Similar fixed phase is observed in the LHD experiments.
- In LHD, a **natural error field** exists, which **works as an RMP**.
The $m=1/n=1$ component is dominant.
This error field can be reduced by controlling the RMP coil currents.
- In either case of the reduction or the existence of the error field, pressure collapses are observed in the configurations similar to the present case.

Mode location in collapses
(toroidal angle where the O-point is located at the mid plane of the low-field side)



(S.Sakakibara et al. NF (2013) 0430101)

- In the **reduction of the error field** case, the mode **locations differ** for every discharge.
- In the **existence of the error field** case, the mode **locations are concentrated** at the phase of the error field.
- This **phase property agrees** with the present numerical results.
- To investigate the detailed mechanism, analyses including RMP penetration and plasma rotation, and precise comparison will be necessary.

- ◆ For MHD analyses of resonant magnetic perturbations (RMPs), 3D equilibrium calculation including RMPs is crucial, because RMPs can change the structure of pressure driven modes through the change of the equilibrium pressure profile.
- ◆ In the case of an LHD plasma, a horizontally uniform RMP changes the mode structure from an interchange type to a ballooning type localized around the X-point.
- ◆ The spatial phase of the nonlinear collapse is fixed corresponding to the geometry of the magnetic island.
- ◆ Similar fixed phase is observed in the LHD experiments with the error field.
- ◆ To investigate the detailed mechanism in the experiments, we need further analyses including RMP penetration and plasma rotation, and precise comparison.